Quantum quench thermodynamics at high temperatures

Adalberto D. Varizi,[1] Raphael C. Drumond,[2] and Gabriel T. Landi[3]
[1]*Departamento de Física, Instituto de Ciências Exatas, Universidade Federal de Minas Gerais, Belo Horizonte, 30123-970 Minas Gerais, Brazil*
[2]*Departamento de Matemática, Instituto de Ciências Exatas, Universidade Federal de Minas Gerais, Belo Horizonte, 30123-970 Minas Gerais, Brazil*
[3]*Instituto de Física da Universidade de São Paulo, São Paulo, 05314-970 São Paulo, Brazil*

(Received 20 September 2021; accepted 10 June 2022; published 29 June 2022)

The entropy produced when a system undergoes an infinitesimal quench is directly linked to the work parameter susceptibility, making it sensitive to the existence of a quantum critical point. Its singular behavior at $T = 0$, however, disappears as the temperature is raised, hindering its use as a tool for spotting quantum phase transitions. Notwithstanding, the entropy production can be split into classical and quantum components, related with changes in populations and coherences. In this paper we show that these individual contributions can continue to exhibit signatures of the quantum phase transition, even at arbitrarily high temperatures. This is a consequence of their intrinsic connection to the derivatives of the energy eigenvalues and the energy eigenbasis. We illustrate our results in the Landau-Zener model and the prototypical quantum critical system, the XY model.

DOI: 10.1103/PhysRevA.105.062218

I. INTRODUCTION

At zero temperature a quantum many-body system can manifest distinct behaviors depending on the values of its internal couplings. And, as these values are altered, quantum fluctuations may drive the system through a phase transition. These quantum phase transitions are characterized by stark modifications in the system's ground state, frequently associated with a symmetry breaking at a critical point.

Such transitions can be characterized with a variety of information theoretic tools, such as ground-state fidelity, fidelity susceptibility, and Loschmidt echo [1]. For finite systems, a large overlap between the ground states of nearby Hamiltonians in parameter space is expected, giving a fidelity close to unity. In contrast, the distinct properties of the ground states pertaining to different phases make them more "distant," and this is revealed as a sharp drop in fidelity in the vicinity of the transition point [2]. Equivalently, this effect can be verified as an increase in the fidelity rate change, the fidelity susceptibility, signaling the existence of a phase transition [1,2].

In a similar way, the Loschmidt echo, which behaves as a type of dynamic fidelity, gives a measure of the distinguishability between the time-evolved ground states of an unperturbed Hamiltonian and its perturbed counterpart. When the system is quenched through a critical point, the echo may have a dip at the critical parameter and a series of decays and revivals as a function of time, also indicating the presence of critical behavior [3,4].

As the temperature T is raised above zero, a competition between quantum and thermal fluctuations emerge, with the latter quickly dominating the physics of the problem [5]. Nonetheless, fingerprints of the quantum critical point are still visible for finite temperatures, albeit not as sharply as at $T = 0$. A generalization of the ground-state fidelity and Loschmidt echo approaches to thermal states was put forward in Ref. [6]. A decay in their values close to the quantum critical point was also observed, although gradually less sharp with rising temperatures, up to a complete disappearance of any distinct feature.

On another front, the correlations and/or coherences in the system have been likewise used as tools for locating transition points. This started with entanglement measures [7,8] (or some derivatives of it), which can show nonanalytic behavior at a quantum critical point. Similar analysis was later extended to mutual information, classical correlations, and quantum discord [9,10], and more recently to quantifiers of coherence [11–17] in several spin models. Commonly, the singularities in these quantities disappear at finite T, and attempts to estimate the critical point from the extrema of these functions generally become poorer with increasing temperature.

An exception, though, was demonstrated in Ref. [18] for quantum discord. In this case, the authors showed that a kink in the discord in the state of two nearest-neighbor spins, reduced from a global thermal state, in the XXZ model with no external field, indicates the quantum critical points in the system even at high temperatures. Still, further analyses with other models [19,20] showed that for some transitions these nonanalyticities can, again, disappear, with the peaks or valleys that replace them becoming less pronounced and displaced from the true critical point with increasing temperature.

Quantum phase transitions have also played a similar role in the context of quantum thermodynamics, particularly in the case of unitary work protocols. In fact, in Refs. [21,22] it was shown that a divergence in the entropy production during a sudden quench pinpointed the existence of a quantum critical point. The entropy production is generally written as a

quantum relative entropy and, therefore, similarly gives a measure of distinguishbility between states. Here, a temperature is naturally introduced from the start, but again, the divergence at $T = 0$ is smoothed as T increases [21].

The entropy production, however, can be consistently split into two parts, associated with classical and quantum contributions, the latter steaming from quantum coherences [23–26]. Beyond unitary work protocols [24], particularly in critical systems [26,27], this type of splitting has found many applications like in work extraction protocols [28], relaxation towards equilibrium [23,29], quasistatic evolution and consequences of coherences to the fluctuation-dissipation theorem [25,30], thermodynamics resource theory [31], and quantum optics thermodynamics [32]. In Refs. [26,27] we hinted at the fact that this contribution could individually signal the existence of a quantum critical point (hence $T = 0$) even with protocols performed at *any temperature*. The aim of this paper is to further explore and clarify this point.

Hence, we consider a system with Hamiltonian $H(g)$, depending on an externally tunable parameter g and initially prepared in a thermal state at temperature $T = 1/\beta$. Thus, the system's initial state is given by $\rho_0^{\rm th} = e^{-\beta H_0}/Z_0$, where $H_0 = H(g_0)$ is the initial Hamiltonian and $Z_0 = \mathrm{tr}\{e^{-\beta H_0}\}$ is the partition function. The system then undergoes a sudden quench work protocol, where g is changed to a final value of g_τ. Since the quench is assumed to be instantaneous, the state of the system remains the same, $\rho_0^{\rm th}$, but its Hamiltonian changes to $H_\tau = H(g_\tau)$. Therefore, the system is driven away from equilibrium. The entropy production (or nonequilibrium lag) due to this process is given by [33,34]

$$\Sigma = S\big(\rho_0^{\rm th}\big|\big|\rho_\tau^{\rm th}\big), \tag{1}$$

where $S(\rho||\sigma) = \mathrm{tr}\{\rho(\ln\rho - \ln\sigma)\} \geqslant 0$ is the quantum relative entropy, and $\rho_\tau^{\rm th} = e^{-\beta H_\tau}/Z_\tau$ is the equilibrium reference state associated with the final Hamiltonian H_τ. The entropy production Σ may also be written in the enlightening form $\Sigma = \beta(\langle W\rangle - \Delta F)$, where $\langle W\rangle = \mathrm{tr}\{(H_\tau - H_0)\rho_0^{\rm th}\} = \mathrm{tr}\{\Delta H\rho_0^{\rm th}\}$ is the average work performed in the protocol and $\Delta F = F(g_\tau) - F(g_0) = -T\ln Z_\tau/Z_0$ is the difference in equilibrium free energy. Due to this thermodynamic interpretation, entropy production has recently been used extensively as a quantifier of irreversibility, in both theory [35–43] and experiment [44–55].

Let us consider the quench $\delta g = g_\tau - g_0$ to be small. Then we can make a Taylor expansion, and the entropy production can be simplified to [25,26]

$$\Sigma = \Lambda_{\rm cl} + \Lambda_{\rm qu}, \tag{2}$$

$$\Lambda_{\rm cl} = \frac{\beta^2}{2}\mathrm{Var}_0[\Delta H^{\rm d}], \tag{3}$$

$$\Lambda_{\rm qu} = \frac{\beta^2}{2}\mathrm{Var}_0[\Delta H^{\rm c}] - \frac{\beta^2}{2}\int_0^1 dy I^y\big(\rho_0^{\rm th}, \Delta H^{\rm c}\big), \tag{4}$$

where $\Delta H^{\rm d}$ is the diagonal part of the perturbation in the basis of H_0 (and $\rho_0^{\rm th}$), $\Delta H^{\rm c} = \Delta H - \Delta H^{\rm d}$ is the coherent part, $\mathrm{Var}_0[(\bullet)] = \mathrm{tr}\{(\bullet)^2\rho_0^{\rm th}\} - \mathrm{tr}\{(\bullet)\rho_0^{\rm th}\}^2$ is the variance of $(\bullet)$ in the initial thermal state, and

$$I^y(\varrho, X) = -\tfrac{1}{2}\mathrm{tr}\{[\varrho^y, X][\varrho^{1-y}, X]\} \tag{5}$$

is the Wigner-Yanase-Dyson skew information [56,57]. The term $\Lambda_{\rm qu}$ quantifies the entropy production associated with the coherences generated by a noncommuting drive. Equations (3) and (4) take into account only the leading contributions on the small perturbation. Importantly, both $\Lambda_{\rm cl}$ and $\Lambda_{\rm qu}$ in Eq. (2) are individually non-negative [26].

Moreover, for sufficiently high temperatures, the splitting (2) coincides with an alternative expansion used in Refs. [23,24], which reads

$$\Sigma = S\big(\mathbb{D}_{H_\tau}\big(\rho_0^{\rm th}\big)\big|\big|\rho_\tau^{\rm th}\big) + S\big(\rho_0^{\rm th}\big|\big|\mathbb{D}_{H_\tau}\big(\rho_0^{\rm th}\big)\big), \tag{6}$$

where $\mathbb{D}_{H_\tau}(\rho_0^{\rm th})$ is the initial state dephased in the final energy basis. Therefore, the first term gives a contribution due to the mismatch between the populations of the initial and final equilibrium states, while the second term gives the contribution to the entropy production stemming from the coherences in $\rho_0^{\rm th}$ in the final energy basis as measured by the relative entropy of coherence [58]. For T values high enough, they coincide with $\Lambda_{\rm cl}$ and $\Lambda_{\rm qu}$ [26], respectively. This means that, in this particular regime of infinitesimal quenches and high temperatures, the splittings (2) and (6) are equivalent.

In what follows, in Sec. II we show why and how $\Lambda_{\rm cl}$ and $\Lambda_{\rm qu}$ can be used to investigate a quantum critical point. Notably, we see that this approach is useful at any temperature. In Sec. III and IV we consider the Landau-Zener and XY models as examples of quantum critical systems to illustrate our results. In Sec. V we discuss how, in principle, these results could be verified experimentally. We conclude in Sec. VI.

II. QUANTUM CRITICAL SIGNATURES AT HIGH TEMPERATURES

We consider a system described by the Hamiltonian

$$H(g) = H_0 + gH_1, \tag{7}$$

where g is an externally adjustable parameter. If the two parts of this Hamiltonian do not commute, $[H_0, H_1] \neq 0$, in the thermodynamic limit the quantum fluctuations induced by H_1 as $|g|$ is raised above zero may cause a continuous (second-order) quantum phase transition in the system at some critical value of g_c. As noted earlier, the existence of this critical point may imprint a signature in physically observable quantities, even if the system is finite in size and/or is at a finite temperature.

Let us assume that $H(g)$ has the following eigendecomposition:

$$H(g) = \sum_i \epsilon_i(g)\,\Pi_i(g), \tag{8}$$

where ϵ_i and Π_i are the energy eigenvalues and eigenprojectors, respectively. These are generally functions of g, and differentiating with respect to it, we get

$$(\partial_g H)\delta g = \delta g\sum_i(\partial_g\epsilon_i)\Pi_i + \delta g\sum_i \epsilon_i(\partial_g\Pi_i). \tag{9}$$

Note that for a system presenting a second-order quantum phase transition, these *first* derivatives may present a kink at a critical point but are still continuous and well-defined functions for all g.

On the other hand, suppose we apply an instantaneous perturbation δg on the system. We have $H(g + \delta g) = H(g) +$

ΔH, where ΔH can be split as

$$\Delta H = \Delta H^{\mathrm{d}} + \Delta H^{\mathrm{c}}, \tag{10}$$

with $\Delta H^{\mathrm{d}} = \sum_i \Pi_i \Delta H \Pi_i$ being the diagonal part of the perturbation in the eigenbasis of the original Hamiltonian $H(g)$, and $\Delta H^{\mathrm{c}} = \Delta H - \Delta H^{\mathrm{d}}$ being the coherent part. Now, because H is continuous and linear on g we must have

$$\Delta H = H(g+\delta g) - H(g) = (\partial_g H)\delta g. \tag{11}$$

Combining Eqs. (9) to (11), we readily find that

$$\Delta H^{\mathrm{d}} = \delta g \sum_i (\partial_g \epsilon_i)\Pi_i, \tag{12}$$

$$\Delta H^{\mathrm{c}} = \delta g \sum_i \epsilon_i (\partial_g \Pi_i). \tag{13}$$

Now consider that we prepare the system in thermal equilibrium, as discussed in Sec. I. For sufficiently high temperatures (small β), the thermal state $\rho_0^{\mathrm{th}} = e^{-\beta H(g_0)}/Z(g_0)$ is close to the maximally mixed state, $\rho_0^{\mathrm{th}} \to \frac{\mathbb{1}}{d}$, where d is the dimension of the system. Such an approximation holds when T (β) is much larger (smaller) than the energy of the highest excitation on the system. For instance, below we consider the example of the one-dimensional XY model, which is mapped onto a system of free fermions. In this case, we must have $\beta\epsilon_{\max} \ll 1$, where $\epsilon_{\max}$ is the energy of the highest fermionic excitation. Further assuming δg is small and $\mathrm{tr}\{\Delta H^{\mathrm{d}}\} = 0$, which can always be done, it is easy to show that to leading order in β, Eqs. (3) and (4) reduce to

$$\Lambda_{\mathrm{cl}} = \frac{\beta^2 \delta g^2}{2} \sum_i \frac{d_i}{d} (\partial_g \epsilon_i)^2, \tag{14}$$

$$\Lambda_{\mathrm{qu}} = \frac{\beta^2 \delta g^2}{2} \sum_i \frac{||\epsilon_i (\partial_g \Pi_i)||^2}{d}, \tag{15}$$

where $d_i = \mathrm{tr}\{\Pi_i\}$ is the dimension of projector Π_i, $||X|| = \sqrt{\mathrm{tr}\{X^\dagger X\}}$ is the Hilbert-Schmidt norm of X, and we also use that ΔH^{c} is traceless, by construction. Corrections to these formulas will be of order β^3 at least and can be safely ignored for small β.

From these results, we therefore see that Λ_{cl} and Λ_{qu} are directly connected to the derivatives of the energy eigenvalues and the energy eigenbasis with respect to the critical parameter of the Hamiltonian. But by definition [5], in the thermodynamic limit, the ground state and the ground-state energy of a quantum critical system are nonanalytic in the vicinity of a critical point. Because of the form of Eqs. (14) and (15), these singularities get imprinted on Λ_{cl} and Λ_{qu} no matter how high the temperature is. Furthermore, since for a system presenting second-order transitions the thermal state ρ_0^{th} is a continuous function of β, the distinct behaviors of Λ_{cl} and Λ_{qu} at the quantum critical point g_c persists at every temperature. Precisely, at any $T > 0$, Λ_{qu} and Λ_{cl} are functions of the first derivatives of the energy eigenvalues and eigenstates multiplied by a continuous function of β steaming from ρ_0^{th}, with continuous first-order derivative. The kinks on the Hamiltonian spectrum at $g = g_c$ are inherited by the classical and quantum parts of the entropy production.

Contrastingly, in the limit $T \to \infty$ ($\beta \to 0$), using also that $\mathrm{tr}\{\Delta H\} = \mathrm{tr}\{\Delta H^{\mathrm{d}}\} = 0$, the total entropy production is simply given by

$$\Sigma = \frac{\beta^2}{2} \mathrm{tr}\left\{\frac{\mathbb{1}}{d} \Delta H^2\right\}. \tag{16}$$

But $\Delta H = \delta g(\partial_g H) = \delta g H_1$, which makes Σ independent of the critical parameter g. This is why in the high-temperature limit the full entropy production can show no singularity at g_c.

Hence, the classical and quantum contributions to the entropy production, Eqs. (3) and (4), can be used to investigate the existence of a second-order quantum critical point at any temperature. We now illustrate this via two analytically soluble examples. Before continuing, though, we emphasize that, since Eqs. (14) and (15) involve a sum over all energy subspaces, we cannot discard the possibility of systems where the singularities in the ground and low-lying levels are too weak and become eroded by this sum. Moreover, it is also possible to have systems where the singularities on Λ_{cl} and Λ_{qu} at high temperatures are inherited from singularities on the middle of the energy spectrum and not necessarily from the ground state. This could be the case, for instance, in a higher-dimensional and nonintegrable model with a critical point at finite T. Due to the eigenstate thermalization hypothesis, high-energy eigenstates would inherit the singularities of the equilibrium states around the critical point [59].

III. LANDAU-ZENER MODEL

The Landau-Zener model is a single-qubit Hamiltonian which can be regarded as a prototype of a quantum critical system [22]. It reads

$$H_{\mathrm{LZ}}(g) = \left(-\frac{\Delta}{2} + g\right)\sigma^z + b\sigma^x, \tag{17}$$

where $\sigma^{x,z}$ are Pauli spin-$\frac{1}{2}$ operators and g represents an externally controlled magnetic field. This system has an avoided crossing at $g_{\mathrm{c}} = \Delta/2$ for $b \to 0$, similar to what happens in a system presenting a second-order quantum phase transition [see Fig. 1(a)]. Importantly, however, we note that since this is a single-qubit system, this is not a real critical system, and there is no real phase transition in this case. The model still neatly illustrates the behaviors of Λ_{qu} and Λ_{cl} as an energy gap closes and how Λ_{qu} and Λ_{cl} capture the associated singularities developed in the spectrum of the system Hamiltonian—contrarily to the case of a real second-order quantum critical point, though, the singularities here occur on the first derivatives of the Hamiltonian eigenstuff.

The Landau-Zener Hamiltonian assumes the following diagonal form:

$$H_{\mathrm{LZ}}(g) = \epsilon(g)\tilde{\sigma}^z, \tag{18}$$

where $\epsilon(g) = \sqrt{b^2 + (g - \Delta/2)^2}$ gives the system eigenenergies, and

$$\tilde{\sigma}^z = |\psi_+\rangle\langle\psi_+| - |\psi_-\rangle\langle\psi_-|, \tag{19}$$

$$|\psi_-(g)\rangle = \cos(\theta/2)|0\rangle - \sin(\theta/2)|1\rangle, \tag{20}$$

$$|\psi_+(g)\rangle = \sin(\theta/2)|0\rangle + \cos(\theta/2)|1\rangle, \tag{21}$$

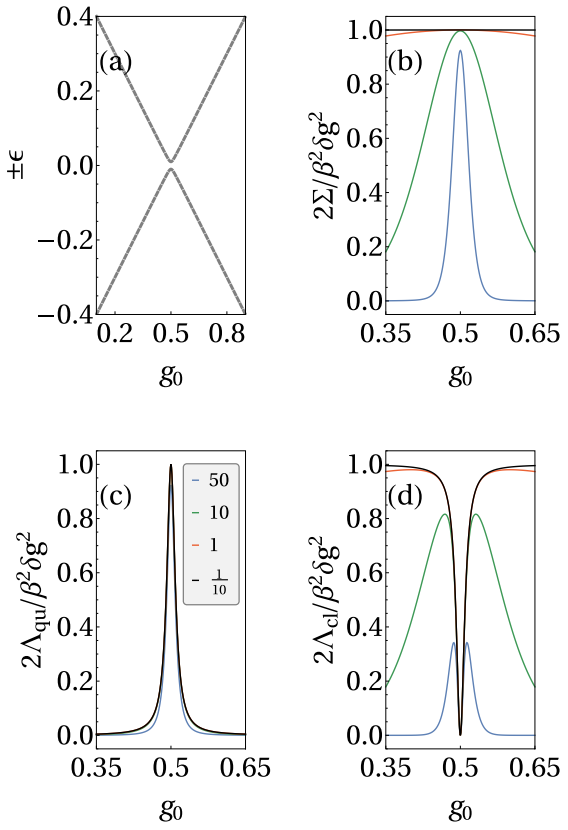

FIG. 1. Landau-Zener model. (a) $\pm\epsilon$ vs g_0, showing the avoided crossing at the critical point $g_0 = 1/2$. (b)–(d) Σ, Λ_{qu}, and Λ_{cl} (scaled by $1/2\beta^2\delta g^2$), for several values of inverse temperatures β, as denoted in panel (c). In Σ, signatures of the transition are only present at low temperatures (high β) and are completely washed away for small β. Conversely, in both Λ_{cl} and Λ_{qu}, clear signatures remain visible over the entire temperature range. Other parameters: $\Delta = 1$ and $b = 0.01$. Note that since the curves are divided by δg^2, we do not need to specify a value for it, just assume it is small enough for Eqs. (3) and (4) to be valid.

$$\big(\cos\theta,\ \sin\theta\big) = \left(\frac{g-\Delta/2}{\epsilon},\ \frac{b}{\epsilon}\right). \tag{22}$$

Here $\sigma^z|i\rangle = (-1)^{i+1}|i\rangle$, $i = 0$ and 1, is the usual computational basis.

For a perturbation $\Delta H = \delta g\sigma^z$, the dephased and coherent parts in the energy eigenbasis read

$$\Delta H^{\rm d} = \delta g(\partial_g\epsilon)\tilde{\sigma}^z = \delta g\cos\theta\,\tilde{\sigma}^z, \tag{23}$$

$$\Delta H^{\rm c} = \delta g\epsilon(\partial_g\tilde{\sigma}^z) = -\delta g\sin\theta\,\tilde{\sigma}^x, \tag{24}$$

where $\tilde{\sigma}^x = |\psi_-\rangle\langle\psi_+| + |\psi_+\rangle\langle\psi_-|$.

The derivatives $\partial_g\epsilon$ and $\partial_g\tilde{\sigma}^z$ are discontinuous at g_c when $b \to 0$, and this is reflected in the behaviors of Λ_{cl} and Λ_{qu} around this point.

Consider a system initially in the thermal state,

$$\rho_0^{\rm th} = \frac{e^{-\beta H_{\rm LZ}(g_0)}}{Z_0} = \frac{e^{-\beta\epsilon^0}|\psi_+^0\rangle\langle\psi_+^0| + e^{\beta\epsilon^0}|\psi_-^0\rangle\langle\psi_-^0|}{2\cosh(\beta\epsilon^0)}, \tag{25}$$

where $\epsilon^0 = \epsilon(g_0)$ and $|\psi_\pm^0\rangle = |\psi_\pm(g_0)\rangle$. Hence, for small δg, using Eqs. (3) and (4), we have

$$\Lambda_{\rm cl} = \frac{1}{2}\beta^2\delta g^2\,{\rm sech}^2(\beta\epsilon^0)\cos^2\theta, \tag{26}$$

$$\Lambda_{\rm qu} = \frac{1}{2}\beta^2\delta g^2\frac{\tanh(\beta\epsilon^0)}{\beta\epsilon^0}\sin^2\theta, \tag{27}$$

which reduce to $\Lambda_{\rm cl} = (1/2)\beta^2\delta g^2\cos^2\theta$ and $\Lambda_{\rm qu} = (1/2)\beta^2\delta g^2\sin^2\theta$ to leading order on β, consistent with Eqs. (14) and (15). In Figs. 1(b)–1(d) we plot Σ, $\Lambda_{\rm qu}$, and $\Lambda_{\rm cl}$ as a function of the initial field for several inverse temperatures β. The net entropy production Σ shows signatures of the closing energy gap at low temperatures. But these are quickly washed away, and for high T (small β) Σ becomes essentially flat. Conversely, the curves for $\Lambda_{\rm qu}$ and $\Lambda_{\rm cl}$ preserve the signatures of the ensuing singularities in the Hamiltonian spectrum for all values of β, indicated by a sharp peak (dip) in the plots of $\Lambda_{\rm qu}$ ($\Lambda_{\rm cl}$) at g_c.

IV. TRANSVERSE FIELD *XY* MODEL

Next, we turn to the transverse field XY model, described by a linear chain with N spins, which has the Hamiltonian

$$H(g,\gamma) = -J\sum_{j=1}^{N}\left(\frac{1+\gamma}{2}\sigma_j^x\sigma_{j+1}^x + \frac{1-\gamma}{2}\sigma_j^y\sigma_{j+1}^y + g\sigma_j^z\right), \tag{28}$$

where $J > 0$ is the ferromagnetic exchange interaction between spins, g is an applied magnetic field, and γ is the anisotropy parameter. We also consider periodic boundary conditions, $\vec{\sigma}_{N+1} = \vec{\sigma}_1$. For $\gamma = 1$, Eq. (28) reduces to the transverse-field Ising model, and $\gamma = 0$ gives the XX model. In the latter, the system eigenbasis is constant (does not depend on g). We henceforth set $J = 1$, thus fixing all other energy units.

Perturbations on the system may be introduced by varying g and/or γ. In the thermodynamic limit, this model presents critical lines at $g = \pm 1$, where the system changes from a ferromagnetic phase, $|g| < 1$, to a paramagnetic phase for $|g| > 1$. There is also an anisotropic transition line at ($\gamma = 0$, $|g| < 1$) where the ferromagnetic ordering changes from the y direction, for $\gamma < 0$, to the x direction, for $\gamma > 0$.

After a Jordan-Wigner transformation that maps the system onto spinless fermions, and a Fourier and Bogoliubov transformations, the Hamiltonian (28) can be written in diagonal form as (we ignore parity issues for simplicity and assume N is even) [5,60]

$$H(g,\gamma) = \sum_k \epsilon_k(2\eta_k^\dagger\eta_k - 1), \tag{29}$$

where $k = \pm(2n+1)\pi/N$, $n = 0, 1, \ldots, N/2-1$, are the system quasimomenta; $\epsilon_k(g,\gamma) = \sqrt{(g-\cos k)^2 + \gamma^2\sin^2 k}$ are the single particle eigenenergies; and

$$\eta_k = \cos(\theta_k/2)c_k + \sin(\theta_k/2)c_{-k}^\dagger, \tag{30}$$

$$(\cos\theta_k, \sin\theta_k) = \left(\frac{g-\cos k}{\epsilon_k(g,\gamma)},\ \frac{\gamma\sin k}{\epsilon_k(g,\gamma)}\right), \tag{31}$$

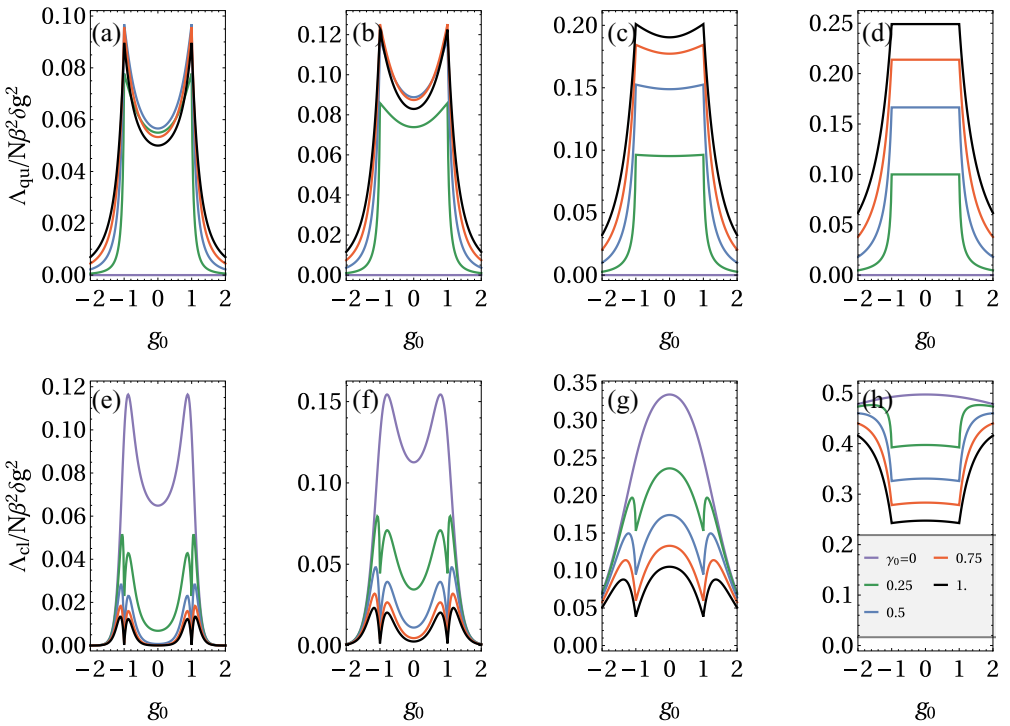

FIG. 2. Plots of Λ_{qu} (top row) and Λ_{cl} (bottom row) as a function of the initial field g_0, scaled by $N\beta^2\delta g^2$, for several values of anisotropy and inverse temperatures: (a) and (e) $\beta = 5$, (b) and (f) $\beta = 3$, (c) and (g) $\beta = 1$, and (d) and (h) $\beta = 0.1$. We consider the anisotropy to be fixed, $\delta\gamma = 0$, and make small quenches δg in the field. Note that when divided by δg^2 the curves are independent of its value. For $\gamma = 0$, the system's eigenbasis is constant and, therefore, $\Lambda_{qu} = 0$. For other values of γ, a kink in both quantities clearly indicates the critical points $g_c = \pm 1$, even at high temperatures. Particularly, in the limit $T \to \infty$ ($\beta \to 0$) we obtain the plateaus and depressions in panels (d) and (h), respectively.

where $\{\eta_k\}$ and $\{c_k\}$ are fermionic operators, satisfying the usual anticommutation relations [5,27]. Note that the set $\{c_k\}$ is independent of g and γ.

For the perturbation $\Delta H = -\delta\gamma/2\sum_{j=1}^{N}(\sigma_j^x\sigma_{j+1}^x - \sigma_j^y\sigma_{j+1}^y) - \delta g\sum_{j=1}^{N}\sigma_j^z$, its dephased and coherent parts were shown in Ref. [26] to be given by

$$\Delta H^{\mathrm{d}} = \sum_k (\delta\gamma \sin k \sin\theta_k + \delta g \cos\theta_k)(2\eta_k^\dagger\eta_k - 1), \quad (32)$$

$$\Delta H^{\mathrm{c}} = \sum_k (\delta g \sin\theta_k - \delta\gamma \sin k \cos\theta_k)(\eta_{-k}^\dagger\eta_k^\dagger - \eta_{-k}\eta_k). \quad (33)$$

Considering the initial thermal state $\rho_0^{\mathrm{th}} = e^{-\beta H_0}/Z_0$, with $H_0 = H(g_0, \gamma_0)$, and performing small sudden quenches δg and $\delta\gamma$, we obtain

$$\frac{\Lambda_{\mathrm{cl}}}{N\beta^2} = \int_0^\pi \frac{dk}{2\pi}\mathrm{sech}^2\left(\beta\epsilon_k^0\right)(\delta\gamma \sin k \sin\theta_k + \delta g\cos\theta_k)^2, \quad (34)$$

$$\frac{\Lambda_{\mathrm{qu}}}{N\beta^2} = \int_0^\pi \frac{dk}{2\pi}\frac{\tanh\left(\beta\epsilon_k^0\right)}{\beta\epsilon_k^0}(\delta g \sin\theta_k - \delta\gamma \sin k\cos\theta_k)^2, \quad (35)$$

where we take the thermodynamic limit $N \to \infty$ to convert the sums over k into integrals, and $\epsilon_k^0 = \epsilon_k(g_0, \gamma_0)$ are the eigenenergies associated with the initial values of anisotropy and field.

Equations (34) and (35) are general expressions for the quench response of Λ_{cl} and Λ_{qu}, valid for any value of β. In Fig. 2 we plot them assuming small quenches δg in the field, with $\delta\gamma = 0$. Each curve corresponds to a value of the anisotropy γ, and each column corresponds to a value of the inverse temperature: (a) and (e) $\beta = 5$, (b) and (f) $\beta = 3$, (c) and (g) $\beta = 1$, and (d) and (h) $\beta = 0.1$. For $\gamma = 0$, the system's constant eigenbasis makes $\Lambda_{\mathrm{qu}} = 0$. In all other curves, there are kinks at $g_0 = \pm 1$, indicating the critical points at high temperatures. In particular, for sufficiently small β we have

$$\frac{\Lambda_{\mathrm{cl}}}{N\beta^2\delta g^2} = \int_0^\pi \frac{dk}{2\pi}\cos^2\theta_k, \quad (36)$$

$$\frac{\Lambda_{\mathrm{qu}}}{N\beta^2\delta g^2} = \int_0^\pi \frac{dk}{2\pi}\sin^2\theta_k, \quad (37)$$

which gives a total entropy production of $\Sigma/N\beta^2\delta g^2 = 1/2$, containing no distinct feature whatsoever. Nonetheless, for $\gamma = 1$, the integral in Eq. (37) evaluates to [27]

$$\frac{\Lambda_{\mathrm{qu}}}{N\beta^2\delta g^2} = \begin{cases} \frac{1}{4}, & |g_0| \leqslant 1, \\ \frac{1}{4|g_0|}, & |g_0| > 1, \end{cases} \quad (38)$$

corresponding to the striking plateaus in the region of parameters associated with the quantum ferromagnetic phase observed in Figs. 2(d) and 2(h). Note that these curves are for $\beta = 0.1$, corresponding to a large temperature. In the Appendix we also analyze the effects of a finite number of spins

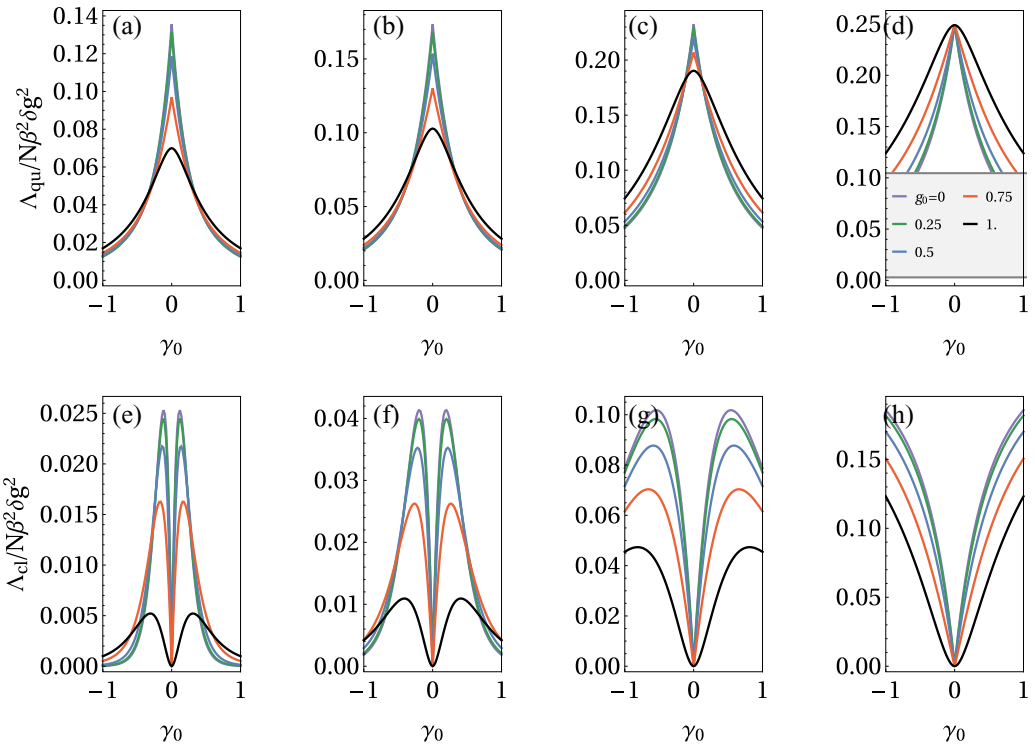

FIG. 3. Analogous to Fig. 2, but analyzing the anisotropic transition. Hence, the quenches are made on the anisotropic parameter, with $\delta g = 0$. Divided by $\delta\gamma^2$, the curves are independent of its value. The peaks in Λ_{qu} above (dips in Λ_{cl} below) evidence the quantum critical line at $\gamma = 0$. Again, each column has an inverse temperature which is equal to the corresponding column in Fig. 2.

N and show that, although the functions become analytic, the thermodynamic limit behavior is quickly approached with increasing N. This mean our analysis could be tested in an Ising model with a relatively small number of spins.

In Fig. 3 we analyze the anisotropic transition by taking $\delta g = 0$ and a small $\delta\gamma$. In this case, each curve corresponds to a value of the transverse field g_0, and, again, each column corresponds to an inverse temperature, with the same values as those in Fig. 2. A cusp in Λ_{cl} and Λ_{qu} at $\gamma_0 = 0$ signals the existence of the quantum critical line associated with the change in the ferromagnetic ordering, even at high temperatures.

V. EXPERIMENTAL ASSESSMENT OF Λ_{cl} AND Λ_{qu}

In this section we propose a way in which the classical and quantum contributions to the entropy production, Λ_{cl} and Λ_{qu}, could, in principle, be evaluated experimentally. Our idea is based on their stochastic formulation using the standard two-point measurement scheme [41] and the fact that they obey fluctuation theorems [26].

The system is initially prepared in the thermal state $\rho_0^{th} = e^{-\beta H_0}/Z_0 = \sum_i (e^{-\beta\epsilon_i^0}/Z_0)|i_0\rangle\langle i_0|$ at inverse temperature β, associated with the Hamiltonian $H_0 = \sum_i \epsilon_i^0 |i_0\rangle\langle i_0|$, which we assume to be nondegenerate, for simplicity. Hence, if we perform an energy measurement in this state, we obtain the energy ϵ_i^0 with the probability $p_i^0 = e^{-\beta\epsilon_i^0}/Z_0$, while the associated measurement backaction updates the state of the system to $|i_0\rangle$. We then perform the quench, and the Hamiltonian changes to the final value $H_\tau = \sum_j \epsilon_j^\tau |j_\tau\rangle\langle j_\tau|$. Since we are considering an instantaneous quench, and given that after the first energy measurement the system is in the state $|i_0\rangle$, a second energy measurement will return the value ϵ_j^τ with the probability $p_{i|j} = |\langle j_\tau|i_0\rangle|^2$.

Therefore, the path probability corresponding to the stochastic trajectory $|i_0\rangle \to |j_\tau\rangle$ is given by the product of the probabilities for the system to be initially found in $|i_0\rangle$ and to transition to the final state $|j_\tau\rangle$, after the quench; it reads $P_F[i, j] = p_i^0 p_{i|j}$. The associated stochastic entropy production is given by [24]

$$\sigma[i, j] = \beta\left(\epsilon_j^\tau - \epsilon_i^0\right) - \beta\Delta F_{\tau,0}, \tag{39}$$

where $w[i, j] = \epsilon_j^\tau - \epsilon_i^0$ is the stochastic work done on the system, and $\Delta F_{\tau,0} = -T \ln Z_\tau/Z_0$ is the change in equilibrium free energy.

It can be readily checked that $\langle\sigma[i, j]\rangle = \sum_{i,j}\sigma[i, j]P_F[i, j] = \Sigma$ gives the expected average (1). Moreover, the quantity σ satisfies an integral fluctuation theorem [61,62], $\langle e^{-\sigma}\rangle = 1$, from which follows the Jarzynski relation $\langle e^{-\beta w[i,j]}\rangle = e^{-\beta\Delta F_{\tau,0}}$ [35].

Thus, we see that if, in an experiment, one can determine the work $w[i, j]$ and the path probability $P_F[i, j]$, $\Delta F_{\tau,0}$ is obtained from the Jarzynski relation and so, finally, is the entropy production Σ. There are several proposals on how this can be done, as well as successful experimental implementations [50,51,63–66]. In Ref. [67] the authors present a general method for obtaining the transition probabilities $p_{i|j}$ in a many-body system and use it to verify the Jarzynski relation for two qubits.

Having said that, next we note that $\Lambda_{\rm cl}$ and $\Lambda_{\rm qu}$ have similar stochastic versions [26],

$$\lambda_{\rm cl}[i,\,j] = \beta\big(\tilde{\epsilon}_i^{\tau} - \epsilon_i^0\big) - \beta\Delta\tilde{F}_{\tau,\,0}, \tag{40}$$

$$\lambda_{\rm qu}[i,\,j] = \beta\big(\epsilon_j^{\tau} - \tilde{\epsilon}_i^{\tau}\big) - \beta\Delta\tilde{F}_{\tau,\,\tau}, \tag{41}$$

where $\tilde{\epsilon}_i^{\tau} = \epsilon_i^0 + \Delta H_{ii} = \epsilon_i^0 + \delta g(\partial_g \epsilon_i^0)$ are the eigenenergies associated with the Hamiltonian $H_0 + \Delta H^{\rm d}$, and $\Delta\tilde{F}_{\tau,0} = -T\ln\tilde{Z}_\tau/Z_0$, with $\tilde{Z}_\tau = {\rm tr}\{e^{-\beta(H_0+\Delta H^{\rm d})}\}$, is the change in the equilibrium free energy due to the incoherent perturbation $\Delta H^{\rm d}$. Additionally, $\Delta\tilde{F}_{\tau,\tau} = -T\ln Z_\tau/\tilde{Z}_\tau$ gives the difference in free energy associated with the perturbation's coherent part $\Delta H^{\rm c}$.

Naturally, we have $\langle\lambda_{\rm cl}\rangle = \sum_{i,j}\lambda_{\rm cl}[i,\,j]P_F[i,\,j] = \Lambda_{\rm cl}$ and $\langle\lambda_{\rm qu}\rangle = \sum_{i,j}\lambda_{\rm qu}[i,\,j]P_F[i,\,j] = \Lambda_{\rm qu}$ [26]. Furthermore, $\lambda_{\rm cl}$ satisfies an integral fluctuation theorem, $\langle e^{-\lambda_{\rm cl}}\rangle = 1$, and this is equally valid for $\lambda_{\rm qu}$ in the infinitesimal and instantaneous quench limit [26].

Now we observe that, up to second order on the perturbation δg, the final energy eigenvalues are given by

$$\begin{aligned}\epsilon_j^{\tau} &= \epsilon_j^0 + \delta g\big(\partial_g\epsilon_j^0\big) + \frac{1}{2}\delta g^2\big(\partial_g^2\epsilon_j^0\big)\\ &= \epsilon_j^0 + \Delta H_{jj} + \frac{1}{2}\sum_{\ell\neq j}\frac{|\Delta H_{j\ell}|^2}{\epsilon_j^0 - \epsilon_\ell^0},\end{aligned} \tag{42}$$

where $\Delta H_{ij} = \langle i_0|\Delta H|j_0\rangle$.

Interestingly, in this limit of instantaneous and infinitesimal quenches, the first term in Eq. (40), $w^{\rm d}[i,\,i] = \tilde{\epsilon}_i^{\tau} - \epsilon_i^0 \approx w[i,\,j]\delta_{ij}$, except in the vicinity of a critical point. In the latter case, the third term in the right-hand side of Eq. (42) can become relevant. Nonetheless, the smaller δg is, the better the approximation and smaller the interval where it breaks down. In the limit $\delta g \to 0$, it should fail only at the critical point. Hence, we can obtain $w^{\rm d}$ from the measured stochastic work w by *postselecting* the cases where the system changes energy without jumping to a state with different label j. Using again a Jarzynski relation, $\langle e^{-\beta w^{\rm d}}\rangle = e^{-\beta\Delta\tilde{F}_{\tau,0}}$, we get $\Delta\tilde{F}_{\tau,0}$, and $\Lambda_{\rm cl} = \beta\langle w^{\rm d}\rangle - \beta\Delta\tilde{F}_{\tau,0}$. From $\Lambda_{\rm cl}$ and Σ, we also obtain $\Lambda_{\rm qu} = \Sigma - \Lambda_{\rm cl}$. This approach, therefore, enables $\Lambda_{\rm qu}$ and $\Lambda_{\rm cl}$ to be determined from the standard two-measurement protocol, provided the data is postselect, which is highly convenient.

VI. CONCLUSION

The entropy production associated with the work done on a closed quantum system can be divided into a classical and a quantum contribution [23–26]. The latter originates from energetic coherences that can be generated by the drive.

In this article we showed that for instantaneous and infinitesimal quenches, these contributions, as given in Eqs. (3) and (4), are respectively and explicitly related to the derivatives of the energy eigenvalues and the energy eigenbasis with respect to the work parameter. In a system presenting a second-order quantum phase transition, one of these energy eigenvalues and eigenstates becomes nonanalytic at a critical point, and this pathology gets engraved on $\Lambda_{\rm cl}$ and $\Lambda_{\rm qu}$. In particular, we demonstrated that their singularities remain present even when the system is prepared at arbitrarily high temperatures. We believe this makes these quantities particularly useful in spotlighting such quantum critical points.

We illustrated this idea by applying our general results to two paradigmatic examples, the Landau-Zener and XY models. The Landau-Zener model is a single-qubit Hamiltonian incorporating an avoided energy crossing, analogous to a second-order quantum phase transition. As a function of the initial work parameter g_0, the entropy production in this model has a peak at the critical point g_c, at low temperatures. As T is raised (or $\beta = 1/T$ is lowered) the relative height (when the curve is divided by β^2) of this peak decreases, and the curve becomes flat in the limit $T \to \infty$ ($\beta \to 0$). The maximum of $\Lambda_{\rm qu}$ (minimum of $\Lambda_{\rm cl}$) at g_c, however, remains present even in this limit. Therefore, $\Lambda_{\rm cl}$ and $\Lambda_{\rm qu}$ can be used to spot the critical point even when the system initially has a high temperature.

In the case of the XY model we considered both the ferromagnetic and the anisotropic transitions. In the former we considered quenches in the field with fixed anisotropy and showed that in the thermodynamic limit $\Lambda_{\rm cl}$ and $\Lambda_{\rm qu}$ per particle have kinks at initial fields equal to the critical values $g_0 = \pm 1$ at all temperatures. Notably, in the limit $T \to \infty$, the total entropy production becomes a constant function of g_0, while $\Lambda_{\rm cl}$ and $\Lambda_{\rm qu}$ present very distinct behaviors in the regions corresponding to different phases, being constant for $|g_0| < 1$ but strictly monotonic when $|g_0| > 1$. In the Appendix, we also considered the effects of a finite chain for the Ising model. Although $\Lambda_{\rm cl}$ and $\Lambda_{\rm qu}$ become analytic in this case, we see the thermodynamic limit behavior is quickly approached with increasing N.

Similarly, considering quenches in the anisotropy, a kink in the curves of $\Lambda_{\rm cl}$ and $\Lambda_{\rm qu}$ at the critical value $\gamma_0 = 0$ signals the presence of the anisotropic critical line at high temperatures.

Finally, we also suggested a way in which these results could be obtained from an experiment. This is based on the stochastic two-point measurement definitions of $\Lambda_{\rm cl}$ and $\Lambda_{\rm qu}$ and the fact that they obey fluctuation theorems. The actual feasibility of our scheme, however, depends on one's ability to determine the stochastic work performed in the protocol and the associated path probabilities.

ACKNOWLEDGMENTS

We acknowledge financial support from the Brazilian agencies Conselho Nacional de Desenvolvimento Científico e Tecnológico (CNPq) and Coordenação de Aperfeiçoamento de Pessoal de Nível Superior, Brasil (CAPES), Finance Code 001. G.T.L. acknowledges the financial support of the São Paulo Funding Agency FAPESP (Grant No. 2019/14072-0.) and the Brazilian funding agency CNPq (Grant No. INCT-IQ 246569/2014-0).

APPENDIX: FINITE-SIZE EFFECTS IN THE ISING MODEL

In this Appendix we consider the effects of a finite number of spins N on the behaviors of $\Lambda_{\rm cl}$ and $\Lambda_{\rm qu}$.

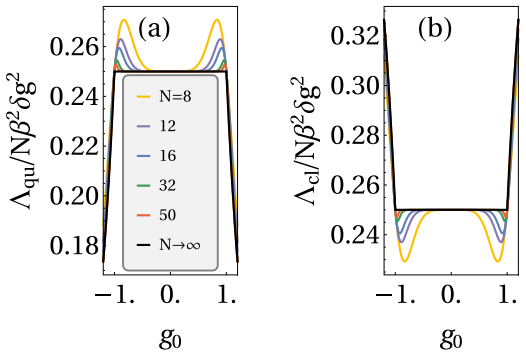

FIG. 4. Plots of (a) Λ_{qu} and (b) Λ_{cl} scaled by $N\beta^2\delta g^2$ as a function of the initial field g_0, for several values of N. The figure shows the limit $N \to \infty$—indicated by the bottom and top flat curve in panels (a) and (b)—is quickly approached with increasing N. We emphasize that we are considering β sufficiently small such that we take only the leading-order contributions.

In particular we take $\gamma = 1$, which means we work with the transverse-field Ising model. We also assume the temperature is high enough so that we can approximate the initial thermal state by the maximally mixed state, $\rho_0^{\text{th}} = \mathbb{1}/2^N$, where 2^N is the dimension of the Hilbert space of a system with N spins. Then, we have

$$\Lambda_{\text{cl}} = \frac{\beta^2}{2}\text{tr}\left\{\frac{\mathbb{1}}{\text{d}}(\Delta H^{\text{d}})^2\right\} = \beta^2\delta g^2 \sum_{k>0}\cos^2\theta_k, \tag{A1}$$

$$\Lambda_{\text{qu}} = \frac{\beta^2}{2}\text{tr}\left\{\frac{\mathbb{1}}{\text{d}}(\Delta H^{\text{c}})^2\right\} = \beta^2\delta g^2 \sum_{k>0}\sin^2\theta_k, \tag{A2}$$

where $k = \pm(2n+1)\pi/N$, n ranging from 0 to $N/2-1$; $\cos\theta_k = (g_0 - \cos k)/\epsilon_k^0$; and $\sin\theta_k = \sin k/\epsilon_k^0$, with $\epsilon_k^0 = \sqrt{(g_0-\cos k)^2 + \sin^2 k}$ and g_0 being the initial field. We also used that $\cos^2\theta_k$ and $\sin^2\theta_k$ are even functions of k.

In Fig. 4 we plot Λ_{cl}/N and Λ_{qu}/N as a function of g_0 for several N. The plots show that the thermodynamic limit behavior (black flat curves) is quickly approximated with increasing N.

This result can be further elucidated as follows. Equations (A1) and (A2) can be recast as

$$\frac{\Lambda_{\text{cl}}}{N\beta^2\delta g^2} = \sum_{k>0}\cos^2\theta_k\frac{\Delta k}{2\pi}, \tag{A3}$$

$$\frac{\Lambda_{\text{qu}}}{N\beta^2\delta g^2} = \sum_{k>0}\sin^2\theta_k\frac{\Delta k}{2\pi}, \tag{A4}$$

where $\Delta k = 2\pi/N$. If we consider a partition,

$$P = \left\{\left[0, \frac{2\pi}{N}\right], \left[\frac{2\pi}{N}, \frac{4\pi}{N}\right], \ldots, \left[\pi - \frac{2\pi}{N}, \pi\right]\right\},$$

of the interval $[0,\pi]$, the right-hand sides of Eqs. (A3) and (A4) are equivalent to midpoint Riemann sums of the functions $\cos^2\theta_k$ and $\sin^2\theta_k$ over $[0,\pi]$ with partition P. The absolute difference between these sums and the respective thermodynamic limit integrals in Eqs. (36) and (37) is bounded by

$$\left|\int_0^\pi \frac{dk}{2\pi}f(k) - \sum_{k>0}f(k)\frac{\Delta k}{2\pi}\right| \leqslant \frac{M\pi^3}{6N^2}, \tag{A5}$$

where $f(k)$ is either $\cos^2\theta_k$ or $\sin^2\theta_k$, and $M = \max_{k\in[0,\pi]}|\partial_k^2 f(k)|$ is the maximum absolute value of the second derivative of $f(k)$ in the interval $[0,\pi]$. Note that f is also a function of the initial field g_0, but we omit this for simplicity of notation. This derivative reads

$$\begin{aligned}\left|\partial_k^2 f(k)\right| = {} & \frac{2}{\left(\epsilon_k^0\right)^4}\left|\sin^2\theta_k\left(g_0^2-1\right)^2\right. \\ & \left. + \epsilon_k^0\cos\theta_k(1-g_0\cos k)\cos k\right|.\end{aligned} \tag{A6}$$

One can graphically check that the maximum of this function occurs at the boundary $k = 0\,(\pi)$ for $g_0 \geqslant 0$ ($g_0 < 0$). Specifically, we have

$$M = \begin{cases}\frac{2}{(g_0+1)^2}, & \text{if } g_0 < 0,\\ \frac{2}{(g_0-1)^2}, & \text{if } g_0 \geqslant 0.\end{cases} \tag{A7}$$

Hence, away from the critical points, the values of Λ_{cl}/N and Λ_{qu}/N for a finite chain converge to the thermodynamic limit with a swiftly decreasing error of order $1/N^2$. The divergence of M at the critical points $g_0 = \pm 1$ also clarifies the slower convergence in these regions.

[1] S.-J. Gu, Int. J. Mod. Phys. B **24**, 4371 (2010).
[2] P. Zanardi and N. Paunković, Phys. Rev. E **74**, 031123 (2006).
[3] H. T. Quan, Z. Song, X. F. Liu, P. Zanardi, and C. P. Sun, Phys. Rev. Lett. **96**, 140604 (2006).
[4] M. Heyl, A. Polkovnikov, and S. Kehrein, Phys. Rev. Lett. **110**, 135704 (2013).
[5] S. Sachdev, *Quantum Phase Transitions* (Cambridge University, Cambridge, England, 2011).
[6] P. Zanardi, H. T. Quan, X. Wang, and C. P. Sun, Phys. Rev. A **75**, 032109 (2007).
[7] A. Osterloh, L. Amico, G. Falci, and R. Fazio, Nature (London) **416**, 608 (2002).
[8] L.-A. Wu, M. S. Sarandy, and D. A. Lidar, Phys. Rev. Lett. **93**, 250404 (2004).
[9] R. Dillenschneider, Phys. Rev. B **78**, 224413 (2008).
[10] M. S. Sarandy, Phys. Rev. A **80**, 022108 (2009).
[11] G. Karpat, B. Çakmak, and F. F. Fanchini, Phys. Rev. B **90**, 104431 (2014).
[12] A. L. Malvezzi, G. Karpat, B. Çakmak, F. F. Fanchini, T. Debarba, and R. O. Vianna, Phys. Rev. B **93**, 184428 (2016).
[13] J.-J. Chen, J. Cui, Y.-R. Zhang, and H. Fan, Phys. Rev. A **94**, 022112 (2016).
[14] Y.-C. Li and H.-Q. Lin, Sci. Rep. **6**, 26365 (2016).
[15] S. Lei and P. Tong, Quantum Inf. Process. **15**, 1811 (2016).
[16] T.-C. Yi, W.-L. You, N. Wu, and A. M. Oleś, Phys. Rev. B **100**, 024423 (2019).

[17] M.-L. Hu, F. Fang, and H. Fan, Phys. Rev. A **104**, 062416 (2021).
[18] T. Werlang, C. Trippe, G. A. P. Ribeiro, and G. Rigolin, Phys. Rev. Lett. **105**, 095702 (2010).
[19] T. Werlang, G. A. P. Ribeiro, and G. Rigolin, Phys. Rev. A **83**, 062334 (2011).
[20] Y.-C. Li and H.-Q. Lin, Phys. Rev. A **83**, 052323 (2011).
[21] R. Dorner, J. Goold, C. Cormick, M. Paternostro, and V. Vedral, Phys. Rev. Lett. **109**, 160601 (2012).
[22] E. Mascarenhas, H. Bragança, R. Dorner, M. França Santos, V. Vedral, K. Modi, and J. Goold, Phys. Rev. E **89**, 062103 (2014).
[23] J. P. Santos, L. C. Céleri, G. T. Landi, and M. Paternostro, npj Quantum Inf. **5**, 23 (2019).
[24] G. Francica, J. Goold, and F. Plastina, Phys. Rev. E **99**, 042105 (2019).
[25] M. Scandi, H. J. D. Miller, J. Anders, and M. Perarnau-Llobet, Phys. Rev. Res. **2**, 023377 (2020).
[26] A. D. Varizi, M. A. Cipolla, M. Perarnau-Llobet, R. C. Drumond, and G. T. Landi, New J. Phys. **23**, 063027 (2021).
[27] A. D. Varizi, A. P. Vieira, C. Cormick, R. C. Drumond, and G. T. Landi, Phys. Rev. Res. **2**, 033279 (2020).
[28] G. Francica, F. C. Binder, G. Guarnieri, M. T. Mitchison, J. Goold, and F. Plastina, Phys. Rev. Lett. **125**, 180603 (2020).
[29] M. H. Mohammady, A. Auffèves, and J. Anders, Commun. Phys. **3**, 89 (2020).
[30] H. J. D. Miller, M. Scandi, J. Anders, and M. Perarnau-Llobet, Phys. Rev. Lett. **123**, 230603 (2019).
[31] M. Lostaglio, D. Jennings, and T. Rudolph, Nat. Commun. **6**, 6383 (2015).
[32] C. Elouard, D. Herrera-Martí, M. Esposito, and A. Auffèves, New J. Phys. **22**, 103039 (2020).
[33] R. Kawai, J. M. R. Parrondo, and C. Van den Broeck, Phys. Rev. Lett. **98**, 080602 (2007).
[34] G. T. Landi and M. Paternostro, Rev. Mod. Phys. **93**, 035008 (2021).
[35] C. Jarzynski, Phys. Rev. Lett. **78**, 2690 (1997).
[36] B. Derrida and J. L. Lebowitz, Phys. Rev. Lett. **80**, 209 (1998).
[37] G. E. Crooks, J. Stat. Phys. **90**, 1481 (1998).
[38] J. Kurchan, J. Phys. A: Math. Gen. **31**, 3719 (1998).
[39] J. Lebowitz and H. Spohn, J. Stat. Phys. **95**, 333 (1999).
[40] S. Mukamel, Phys. Rev. Lett. **90**, 170604 (2003).
[41] P. Talkner, E. Lutz, and P. Hänggi, Phys. Rev. E **75**, 050102(R) (2007).
[42] S. Deffner and E. Lutz, Phys. Rev. Lett. **105**, 170402 (2010).
[43] G. Guarnieri, N. H. Y. Ng, K. Modi, J. Eisert, M. Paternostro, and J. Goold, Phys. Rev. E **99**, 050101(R) (2019).
[44] J. Liphardt, S. Dumont, S. B. Smith, I. Tinoco, and C. Bustamante, Science (New York, NY) **296**, 1832 (2002).
[45] F. Douarche, S. Ciliberto, A. Petrosyan, and I. Rabbiosi, Europhys. Lett. **70**, 593 (2005).
[46] D. Collin, F. Ritort, C. Jarzynski, S. B. Smith, I. Tinoco, and C. Bustamante, Nature (London) **437**, 231 (2005).
[47] T. Speck, V. Blickle, C. Bechinger, and U. Seifert, Europhys. Lett. **79**, 30002 (2007).
[48] O. P. Saira, Y. Yoon, T. Tanttu, M. Möttönen, D. V. Averin, and J. P. Pekola, Phys. Rev. Lett. **109**, 180601 (2012).
[49] J. V. Koski, T. Sagawa, O. P. Saira, Y. Yoon, A. Kutvonen, P. Solinas, M. Möttönen, T. Ala-Nissila, and J. P. Pekola, Nat. Phys. **9**, 644 (2013).
[50] T. B. Batalhão, A. M. Souza, L. Mazzola, R. Auccaise, R. S. Sarthour, I. S. Oliveira, J. Goold, G. De Chiara, M. Paternostro, and R. M. Serra, Phys. Rev. Lett. **113**, 140601 (2014).
[51] S. An, J.-N. Zhang, M. Um, D. Lv, Y. Lu, J. Zhang, Z.-Q. Yin, H. T. Quan, and K. Kim, Nat. Phys. **11**, 193 (2014).
[52] T. B. Batalhão, A. M. Souza, R. S. Sarthour, I. S. Oliveira, M. Paternostro, E. Lutz, and R. M. Serra, Phys. Rev. Lett. **115**, 190601 (2015).
[53] M. A. A. Talarico, P. B. Monteiro, E. C. Mattei, E. I. Duzzioni, P. H. Souto Ribeiro, and L. C. Céleri, Phys. Rev. A **94**, 042305 (2016).
[54] Z. Zhang, T. Wang, L. Xiang, Z. Jia, P. Duan, W. Cai, Z. Zhan, Z. Zong, J. Wu, L. Sun, Y. Yin, and G. Guo, New J. Phys. **20**, 085001 (2018).
[55] A. Smith, Y. Lu, S. An, X. Zhang, J.-N. Zhang, Z. Gong, H. T. Quan, C. Jarzynski, and K. Kim, New J. Phys. **20**, 013008 (2018).
[56] E. P. Wigner and M. M. Yanase, Proc. Natl. Acad. Sci. USA **49**, 910 (1963).
[57] A. Wehrl, Rev. Mod. Phys. **50**, 221 (1978).
[58] T. Baumgratz, M. Cramer, and M. B. Plenio, Phys. Rev. Lett. **113**, 140401 (2014).
[59] We thank an anonymous referee for pointing that out.
[60] B. Damski and M. M. Rams, J. Phys. A: Math. Theor. **47**, 025303 (2014).
[61] M. Esposito, U. Harbola, and S. Mukamel, Rev. Mod. Phys. **81**, 1665 (2009).
[62] M. Campisi, P. Hänggi, and P. Talkner, Rev. Mod. Phys. **83**, 771 (2011).
[63] R. Dorner, S. R. Clark, L. Heaney, R. Fazio, J. Goold, and V. Vedral, Phys. Rev. Lett. **110**, 230601 (2013).
[64] L. Mazzola, G. De Chiara, and M. Paternostro, Phys. Rev. Lett. **110**, 230602 (2013).
[65] A. J. Roncaglia, F. Cerisola, and J. P. Paz, Phys. Rev. Lett. **113**, 250601 (2014).
[66] F. Cerisola, Y. Margalit, S. MacHluf, A. J. Roncaglia, J. P. Paz, and R. Folman, Nat. Commun. **8**, 1241 (2017).
[67] M. Herrera, J. P. S. Peterson, R. M. Serra, and I. D'Amico, Phys. Rev. Lett. **127**, 030602 (2021).